

Horizontal Connections for Precast Concrete Shear Walls Subjected to Cyclic Deformations Part 1: Mild Steel Connections

Khaled A. Soudki, Ph.D.

NSERC Post-Doctoral Fellow
Department of Civil Engineering
Queen's University
Kingston, Ontario, Canada



Experimental results of six full-scale specimens tested to investigate the behavior of mild steel connections for precast concrete shear wall panels are presented. The specimens were subjected to reversed cyclic combined flexure and shear in addition to constant axial stresses normal to the connection. The influence of cyclic vs. static loading, mechanical splicing vs. welding of reinforcement, and mechanical splicing vs. bolting of reinforcement to a tube section are discussed. Effects of the use of shear keys and partial debonding of reinforcement on the behavior of the connection are also presented. A simple analytical procedure is developed to predict the envelope of the cyclic response. Based on the findings, design recommendations for mild steel connections of precast concrete walls in seismic zones are presented. A numerical design example is included to show the application of the proposed design procedure.



Sami H. Rizkalla Ph.D., P.Eng.

Professor
Department of Civil and
Geological Engineering
University of Manitoba
Winnipeg, Manitoba, Canada

Bill LeBlanc, P.Eng.

Engineering Manager
ConForce Structures Limited
Winnipeg, Manitoba, Canada



The precast concrete shear wall panel system is a popular structural system in North America for low, medium and high rise residential construction due to its economical advantages. At present, the use of such a system is limited in seismically active regions due to the lack of knowledge of how this type of construction performs under seismic loading conditions.

Table 1. Various types of connections used in test program.

Connection type	Specimen description	Test method
RS-S	Reinforcing bar with NMB splice sleeve	Monotonic
RS	Reinforcing bar with NMB splice sleeve	Cyclic
RSK	Reinforcing bar with NMB splice sleeve and shear keys	Cyclic
RSU	Partially unbonded reinforcing bar with NMB splice sleeve	Cyclic
RW	Reinforcing bar welded to steel angle	Cyclic
RT	Reinforcing bar bolted to HSS tube section	Cyclic

The seismic behavior of a precast concrete structure depends significantly on the connections between the precast elements. Current design codes do not specifically address the seismic design of precast wall connections. In addition, little or no information is available in the existing literature regarding the cyclic behavior of such connections.^{1,2} Therefore, for the precast concrete shear wall system to gain acceptance and be a competitive construction system in seismic regions, the cyclic behavior of connec-

tions between precast members must be addressed.

To achieve this goal, an extensive multi-phase experimental program, undertaken at the University of Manitoba, investigated the behavior of horizontal connections for precast concrete shear wall panels subjected to large reversed cyclic inelastic deformations.³ This program is a continuation of the work conducted to study the behavior of typical precast shear wall connections subjected to monotonic shear.^{4,5,6}

This paper discusses the cyclic shear and cyclic combined flexural and shear behavior of typical and new mild steel connections. The behavior of prestressed connections under similar loading conditions will be presented in a companion paper.

RESEARCH SIGNIFICANCE

This research investigated the behavior of mild steel connections for precast concrete shear walls subjected to reversed cyclic combined flexure and shear in the presence of axial stresses normal to the connection to simulate gravity loads.

The test results were used to determine the strength, stiffness, ductility, energy dissipation, modes of failure, and contribution of each component of the connection to the overall behavior. A simple analytical procedure is proposed to predict the envelope of the

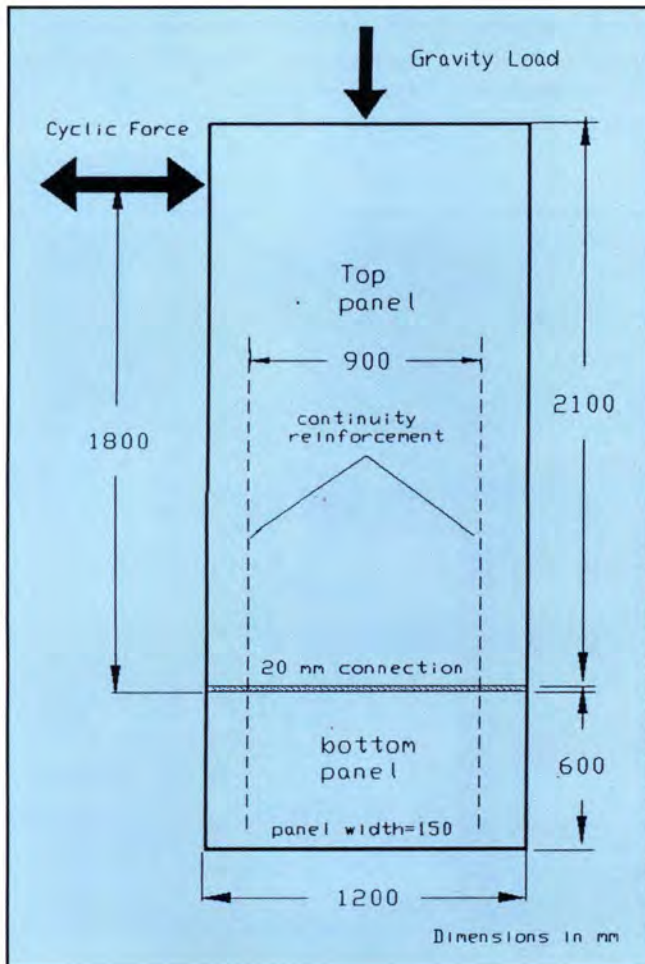


Fig. 1(a). Load arrangement of test specimen.



Fig. 1(b). Test specimen.

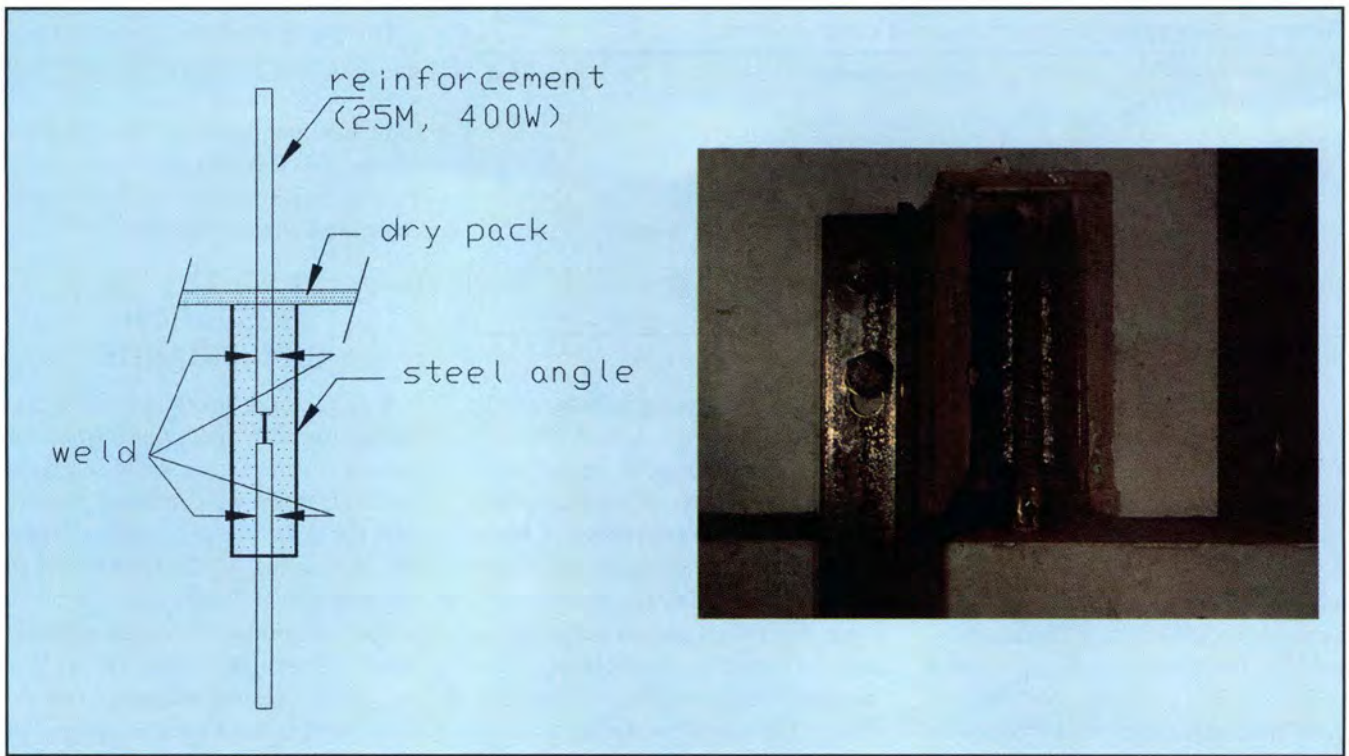


Fig. 2(a). Connection configuration: Type RW.

cyclic response. To illustrate the application of the design procedure, a numerical design example is included. The predicted results compared favorably with the measured values of the research program.

EXPERIMENTAL PROGRAM

Six full-scale mild steel specimens with five different connection configurations were tested in this experimental program under the effect of flexural

and shear loading acting concurrently with constant axial stresses normal to the connection to simulate gravity loading conditions. Five specimens were tested under reversed cyclic loading and one specimen was tested

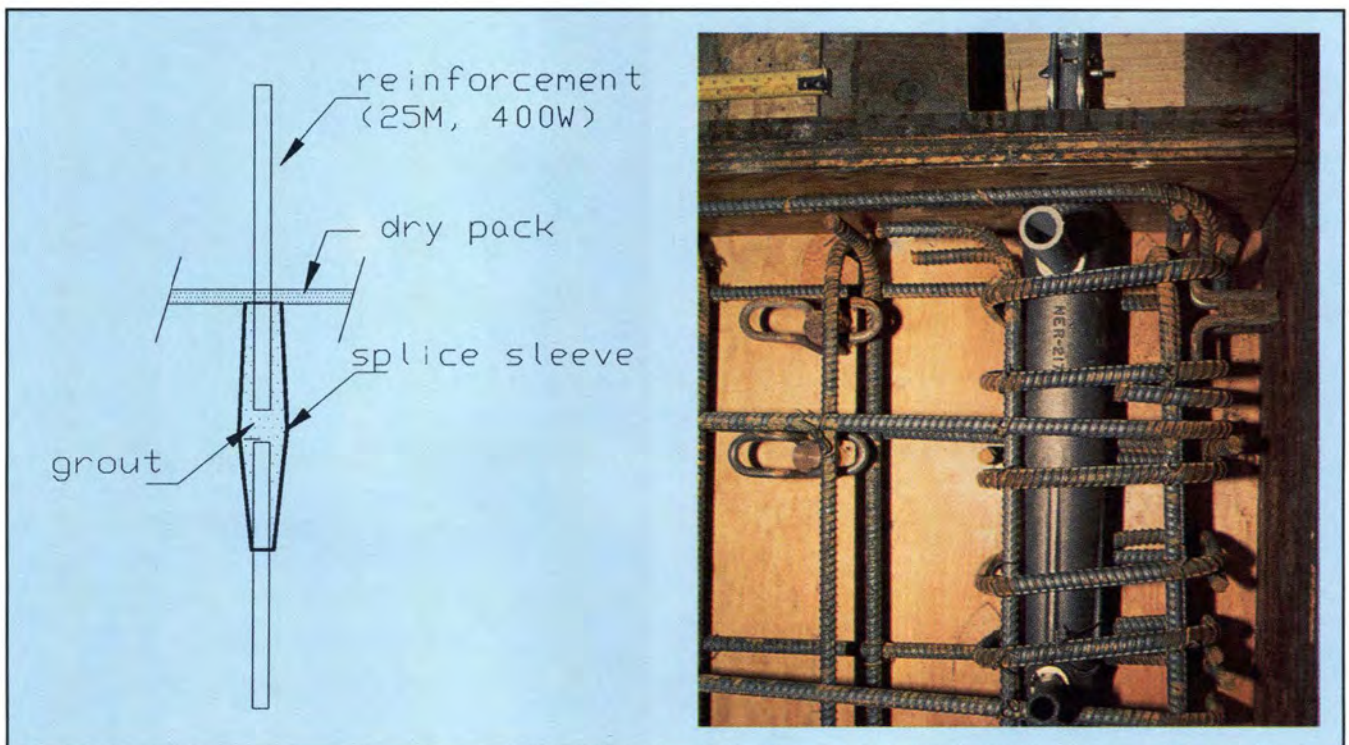


Fig. 2(b). Connection configuration: Types RS and RSU.

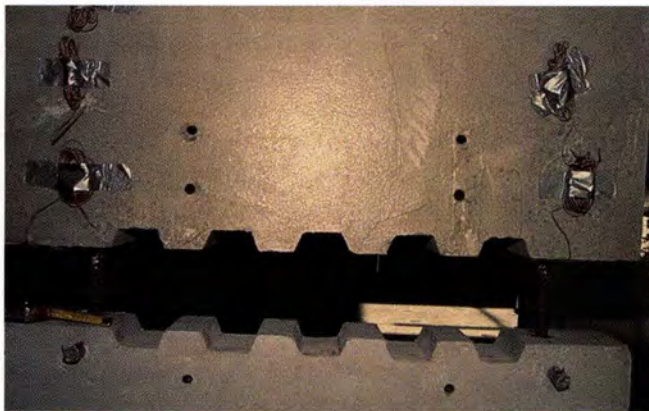
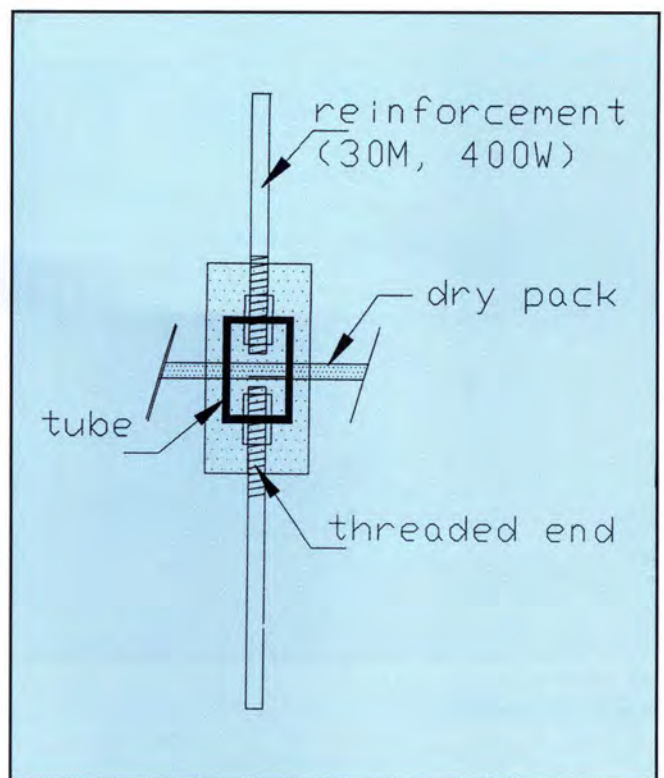
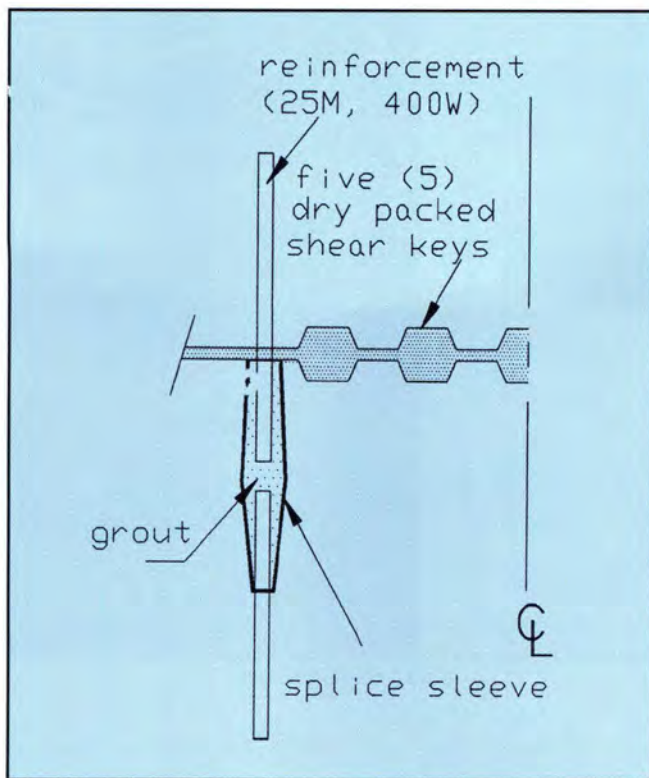


Fig. 2(c). Connection configuration: Type RSK.

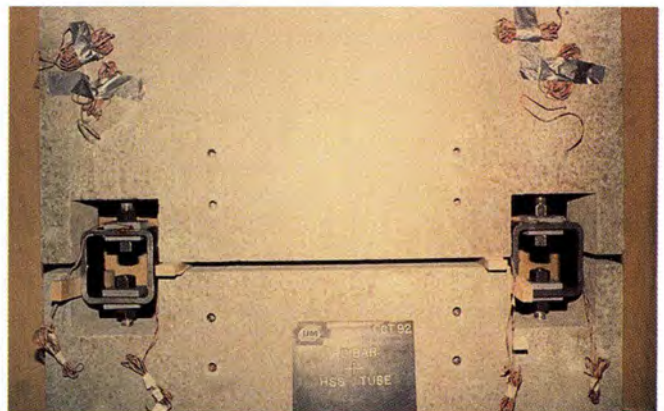


Fig. 2(d). Connection configuration: Type RT.

under monotonic loading to determine the static behavior. Table 1 describes the various types of connections used in the test program.

Test Specimen

The test specimen was selected to simulate horizontal connections near the base of typical shear walls at elevator shafts of a 10-story precast wall building. The specimen consisted of two precast concrete wall panels joined by a horizontal connection, as shown in Fig. 1. The horizontal connection was reinforced by two continuity reinforcing bars and a gap between the precast concrete panels was filled with drypack. The gap between

the panels, in actual structures, is used for alignment purposes.

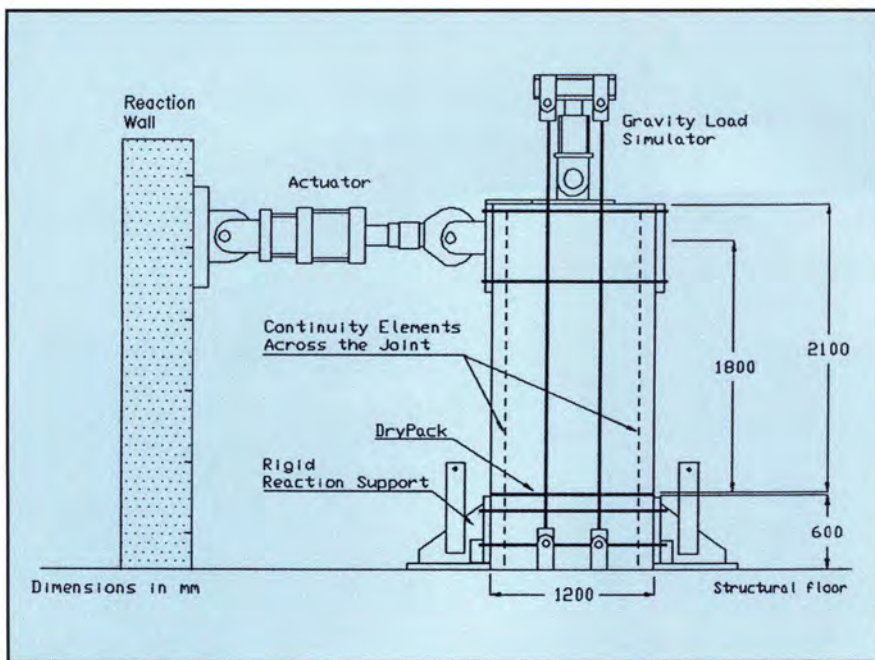
The concrete for the precast panels had a specified nominal strength of 40 MPa (5.8 ksi) at 28 days with a maximum aggregate size of 19 mm ($\frac{3}{4}$ in.) and a slump of 85 mm (3.3 in.). The drypack, between the precast panels, is a zero slump mixture of sand, normal portland cement, and water (2:1:0.2 by weight). The measured average compressive strength of the drypack used, determined using 50 mm (1.97 in.) cubes, is 57 MPa (8.26 ksi).

The connection geometry is 1200 mm (47.25 in.) long, 152 mm (6 in.) wide and 20 mm (0.78 in.) thick, and is identical for all the tested specimens. The continuity between the pan-

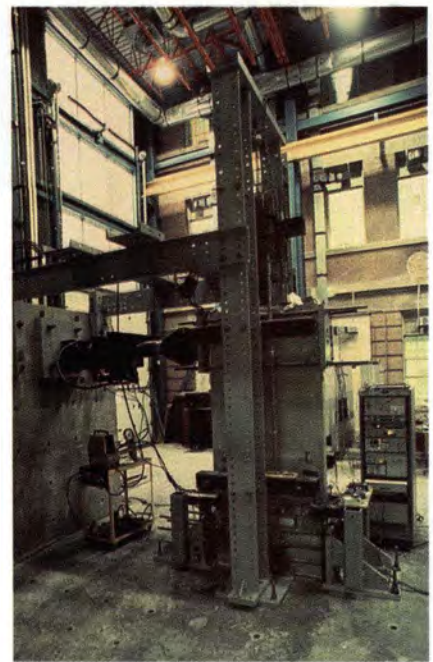
els was provided by two 25.4 mm (1 in.) diameter Grade 400 (60 ksi) reinforcing bars spaced at 900 mm (35.4 in.) center to center.

All the configurations consisted of plain surface panels at the connection region, with the exception of one configuration using multiple shear key surfaces. The different configurations, shown in Fig. 2, are as follows:

RW, reinforcing bars welded to a steel angle — This connection is commonly used by the Canadian precast concrete industry. The protruded straight continuity bar from the top panel is welded to a 75 x 75 x 10 mm (3 x 3 x 0.4 in.) iron angle in an exposed pocket in the lower panel. After welding, the gap between the panels is



(a) Schematic
Fig. 3. Test setup.



(b) Photographic

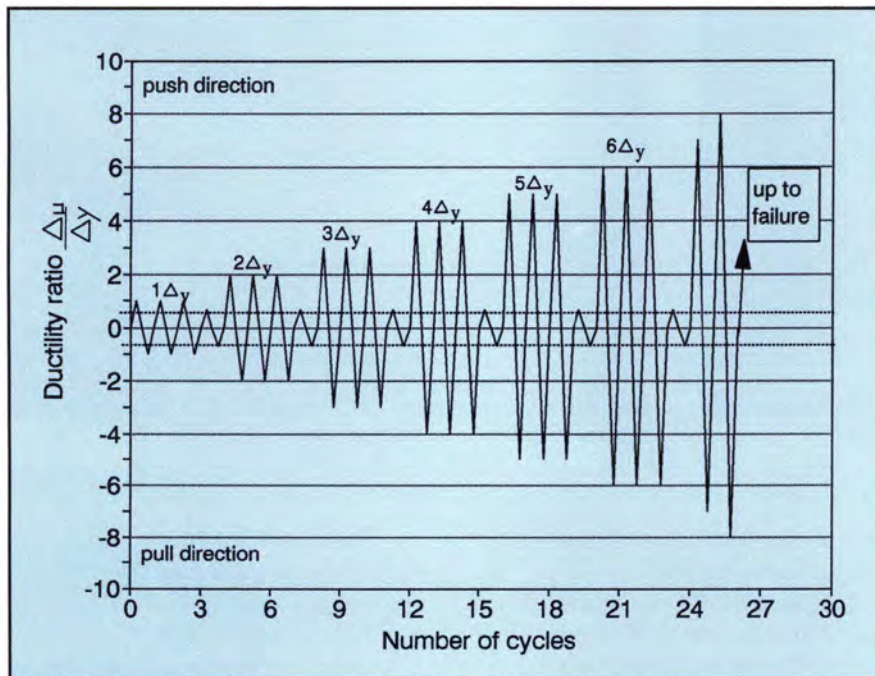


Fig. 4. Reversed displacement control cyclic history.

filled and compacted with drypack, as shown in Fig. 2(a).

RS, reinforcing bars spliced by a sleeve — This connection is typically used by the American and Japanese precast concrete industries. The continuity bars are connected by NMB splice sleeves, as shown in Fig. 2(b). The protruded straight bar from the top panel is placed inside the splice

sleeve, which is embedded in the lower panel. The connection is dry-packed and the splice sleeves are pressure grouted with a non-shrink, high strength, SS mortar.

RSU, reinforcing bars spliced by a sleeve and partially unbonded — This connection is based on a new concept. The overall configuration is identical to Connection RS, with the

exception that a length of the reinforcement in the upper panel is unbonded from the surrounding concrete. This partial unbonding is achieved by applying plastic sheathing on the given length of the bar prior to casting of concrete. The selected unbonded length is 600 mm (23.6 in.) above the connection region.

RSK, reinforcing bars spliced by a sleeve and multiple shear keys — The interface surface of the panel at the connection zone consists of five shear keys, as shown in Fig. 2(c). The length of the shear key is 100 mm (3.94 in.), the depth is 35 mm (1.38 in.) and the sides of the key are inclined at 23 degrees from the vertical. Continuity between the precast panels is achieved by continuity bars connected by means of a splice sleeve, as in Connection RS. The gap between the panels and shear keys is drypacked.

RT, reinforcing bars bolted to a tube — The connection has a plain surface region and continuity is provided by bolting the threaded end of the steel reinforcement to a 152 x 152 x 12.7 mm (6 x 6 x 1 in.) hollow structural steel (HSS) tube placed in rectangular keys at the ends of the connection, as shown in Fig. 2(d). The connection is completed by drypacking the plain surface region and the two tube pockets.

Table 2. Summary of response quantities for mild steel connections.

Specimen	Maximum strength (kN-m)	Yield displacement Δ_y (mm)	Ductility μ_Δ	Drift Δ_u/H (percent)	Stiffness, K (kN/mm)		Slip/displacement S_u/Δ_u (percent)
					K_y	K_u/K_y (percent)	
RS-S	495	4.0	9	2	65	-	13.6
RS	486	4.25	5	1.18	50	20	17.8
RSK	500	4.5	4	1	47.5	30	7.0
RSU	464	6.5	6	2.16	34	22	25
RW	437	5.0	5	1.39	39	20	35
RT	369	4.5	4	1	35	25	17.8

Note: 1 kip = 4.448 kN; 1 in. = 25.4 mm.

Each configuration was tested under reversed cyclic combined flexure and shear loading conditions. In addition, Connection RS was also tested monotonically to determine the monotonic behavior of such connections.

Test Setup and Test Procedure

The test setup used in this experimental program is shown in Fig. 3. The bottom wall panel of the specimen was fixed to the rigid floor by a post-tensioning system against two abutments located at each end of the lower panel. The moment, M , and horizontal shear, V , were applied using a 1000 kN (220 kips) capacity MTS closed loop cyclic actuator by means of a push/pull-type loading yoke located across the top panel at 1800 mm (70.8 in.) above the joint region. This configuration was designed to provide an applied M/VL ratio of 1.5 along the length of the connection, L , for all specimens. This ratio is a typical value for connections near the base of a 10-story precast concrete shear wall building.

The vertical axial stress normal to the joint was applied using an independent prestressing system with swivel pin supports designed to allow displacements in the direction of applied load.

The specimen was instrumented to measure the applied load and to monitor the following response: (1) overall top to bottom panel displacement, Δ , measured at the location of applied load and relative to the bottom fixed panel; (2) local deformations across the joint including panel-to-panel slip, Δ_s , and rocking deformation, Δ_r ; and (3) strains, ϵ , in the reinforcement.

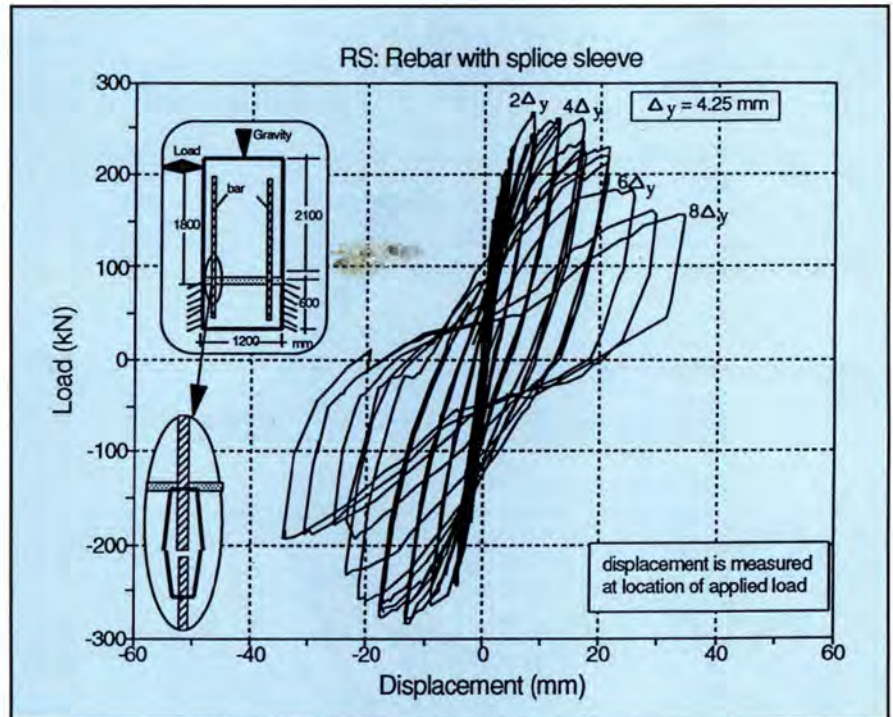


Fig. 5(a). Hysteresis loops of behavior of Specimen RS.

At the beginning of each test, the specimen was loaded to an axial stress of 2 MPa (0.29 ksi) that was held constant for the entire test duration. The test proceeded by applying a controlled series of quasi-static reversed cyclic loading pattern with three cycles at each level.

Initially, the load was applied using load increments equivalent to 25 percent of the estimated yield strength of the connection. Subsequently, the specimen was subjected to displacement cycles at multiples of the yield displacement until failure, as shown in Fig. 4. The test was terminated when the load carrying capacity was reduced by 20 percent of the maximum measured load.

TEST RESULTS

The overall connection behavior of the five connection configurations tested under cyclic loading is given by load-displacement hysteresis loops in Figs. 5(a) through 5(e). The load-displacement behavior of the connection subjected to monotonic loading is given in Fig. 10, which compares the static vs. envelope of cyclic response.

In general, Figs. 5(a) to 5(e) indicate that all the precast specimens subjected to cyclic load exhibited "stable hysteresis" behavior until the onset of failure, followed by pinched loops during post-failure cycles.

Table 2 summarizes the test results for this program. In this paper, the duc-

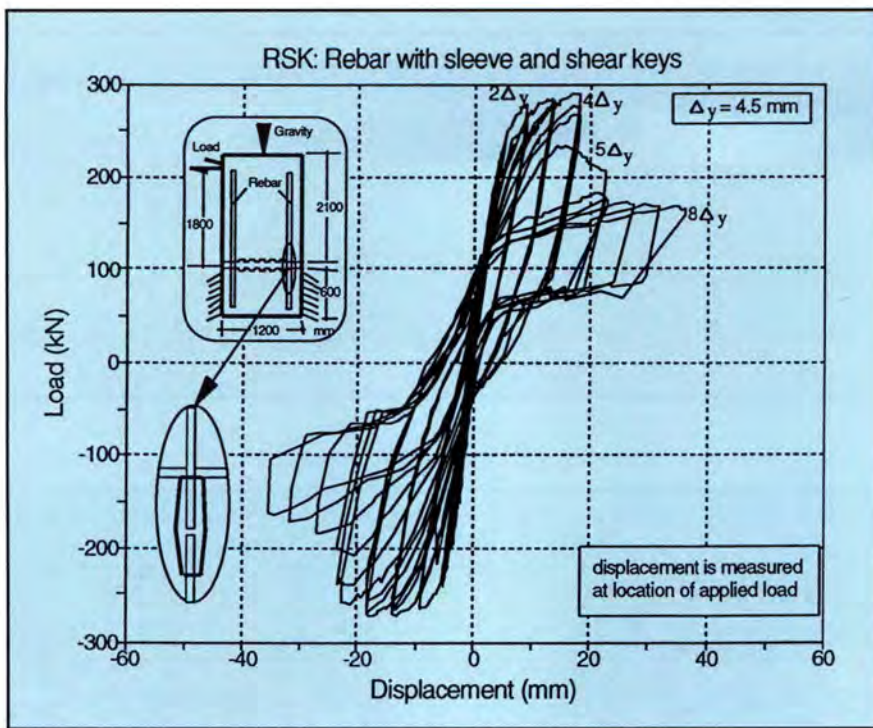


Fig. 5(b). Hysteresis loops of behavior of Specimen RSK.

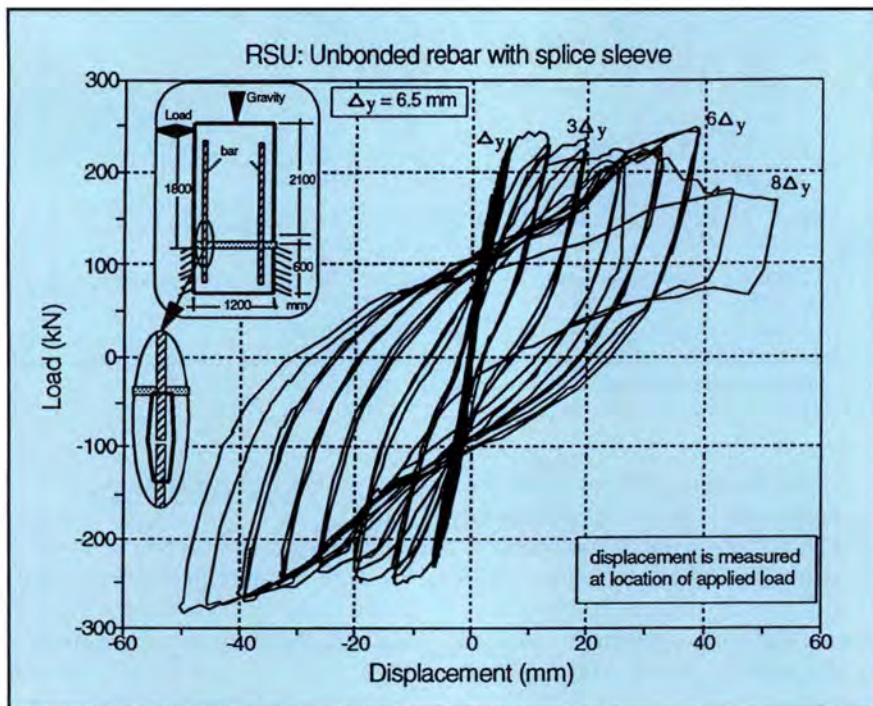


Fig. 5(c). Hysteresis loops of behavior of Specimen RSU.

ility ratio is defined as the ratio of the total displacement, Δ , to displacement at yield, Δ_y . The drift is defined as the ratio of the total displacement, Δ , to the height of the wall panel above the connection region, H , and the rotation is the ratio of the flexural displacement, $\Delta - \Delta_p$, to the height of wall panel.

The behavior of the connection under cyclic loading can be characterized by three distinct limit states depending on the degree of joint deterioration:

1. Elastic stage (less than $1\Delta_y$): prior to yielding of reinforcement without any visible damage.
2. Inelastic ductile stage ($1\Delta_y$ to

$5\Delta_y$): post-yield with nearly stable hysteresis and minor damage without significant joint deterioration.

3. Failure stage ($5\Delta_y$ to $8\Delta_y$): with significant reduction in load carrying capacity under increased deformation. This stage was characterized by severe deterioration of the drypack and rupture or pull-out of the reinforcement from the sleeve.

Rocking Behavior

The rocking behavior is characterized by continuous opening and closing of the joint initially with limited slip. All five connections had similar rocking characteristics with linear displacement-rotation relationships which implies rigid body motion of the top panel relative to the bottom panel. Among the different connections, Connection RSU exhibited approximately twice the magnitude of rotation in comparison to Connection RS before failure.

Reduction of Connection Thickness

Permanent deterioration due to crushing and spalling of drypack along the connection length was observed for all specimens with a plain surface. The degree of deterioration varied from: (1) severe, within the range of 35 to 45 percent reduction of the initial thickness, for Connections RSU and RW due to their large deformation capability; (2) moderate, about 5 percent, for Connection RS; (3) minor, less than 1 percent, for Connection RT due to buckling of the tube at the lower deformation level; and (4) no deterioration, for Connection RSK because the shear keys remained intact during cyclic loading and the crushing was concentrated only at the ends of the panels.

No thickness reduction was measured for Specimen RS-S tested under monotonic loading conditions due to the lack of grinding action typically induced by cyclic loading. Crushing was concentrated only at the compression zone.

Slip Behavior

Slip of the plain surface connections was very similar. At the initial stage of loading, the response was mainly rocking with minor slip. The slip was fully recoverable when the applied

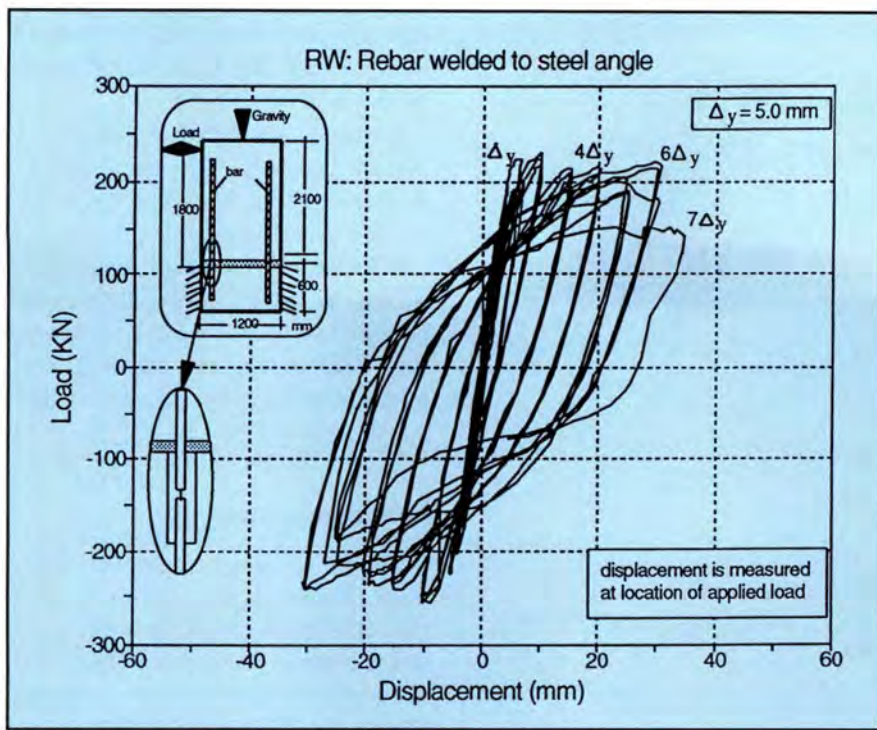


Fig. 5(d). Hysteresis loops of behavior of Specimen RW.

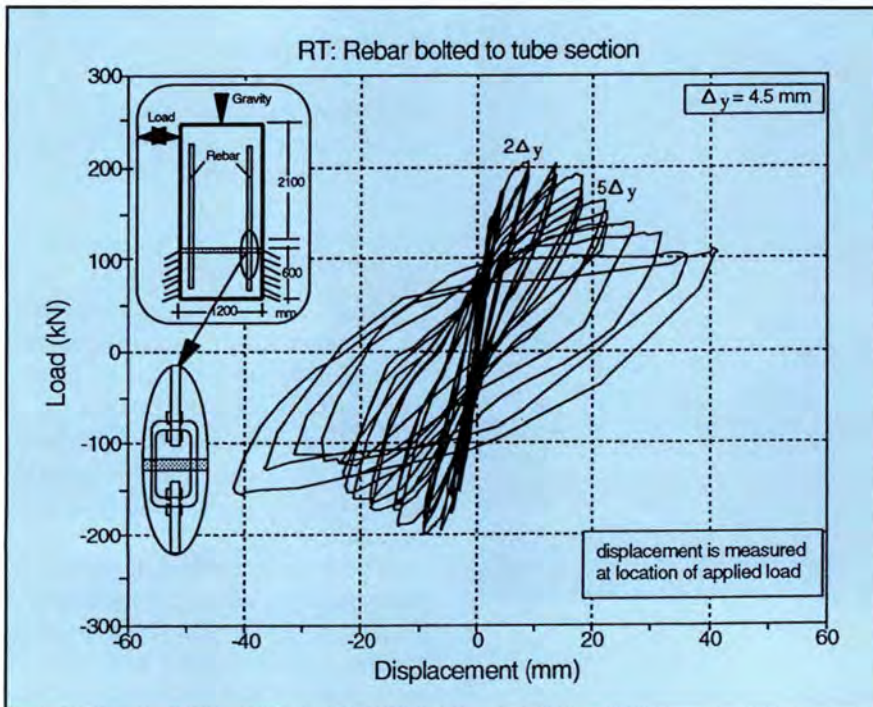


Fig. 5(e). Hysteresis loops of behavior of Specimen RT.

displacement returned to zero. At large displacements, the slip was moderate to major. The magnitude of slip was in proportion to the amount of drypack deterioration.

At onset of failure, the slip hysteresis loops for the plain surface connections were "fat" and reflected an ir-

recoverable mechanism with permanent residual slip at zero displacement.

On the other hand, the multiple shear key connections exhibited consistently narrow slip hysteresis loops at all ductility levels. The slip was minor and fully recoverable when the applied displacement returned to zero.

As the load increased, the percentage of maximum slip, S , to the displacement, Δ , relative to the ductility ratio is shown in Fig. 6. The S/Δ ratios were within the range of 12 to 18 percent for all connections at a ductility ratio of 4 with the exception of a lower ratio of 6 percent for Connection RSK. High S/Δ ratios within the range of 25 and 35 percent were observed for Connections RSU and RW due to the high ductility ratios of 6 and 5 achieved by these configurations, respectively. The slip-to-displacement ratios at ultimate for all specimens are given in Table 2.

Failure Modes

The degree and extent of damage observed at failure varied among the tested specimens, as shown in Fig. 7.

Minor damage was observed for Specimen RS-S tested under monotonic loading. The specimen achieved a ductility ratio of 9 and maximum drift of 2 percent. Crushing of the drypack was concentrated at the extreme end region of the connection; the bulk of the drypack in the compression zone was still intact while the drypack at the outer edges was spalled off. Failure of the connection was due to pull-out of the continuity reinforcement from the sleeve.

Specimen RS had moderate damage across the connection length at a drift of 1.18 percent, and ductility of 5. The specimen failed by pull-out of the bar, which occurred after reaching strain levels corresponding to rupture of the bar. Crushing of the drypack was concentrated at the end region of the connection, around one-third of the connection length, and was ground to a very thin layer. Few compression cracks were observed at the concrete panels within the vicinity of the connection region.

Major damage was observed for Specimen RSU at a drift level of 2.16 percent and ductility of 6. The severe drypack deterioration occurred over the entire connection length at failure due to the high deformation capacity achieved by this type of connection, as shown in Fig. 7(a). The drypack was literally ground to dust in the connection region. Failure was due to pull-

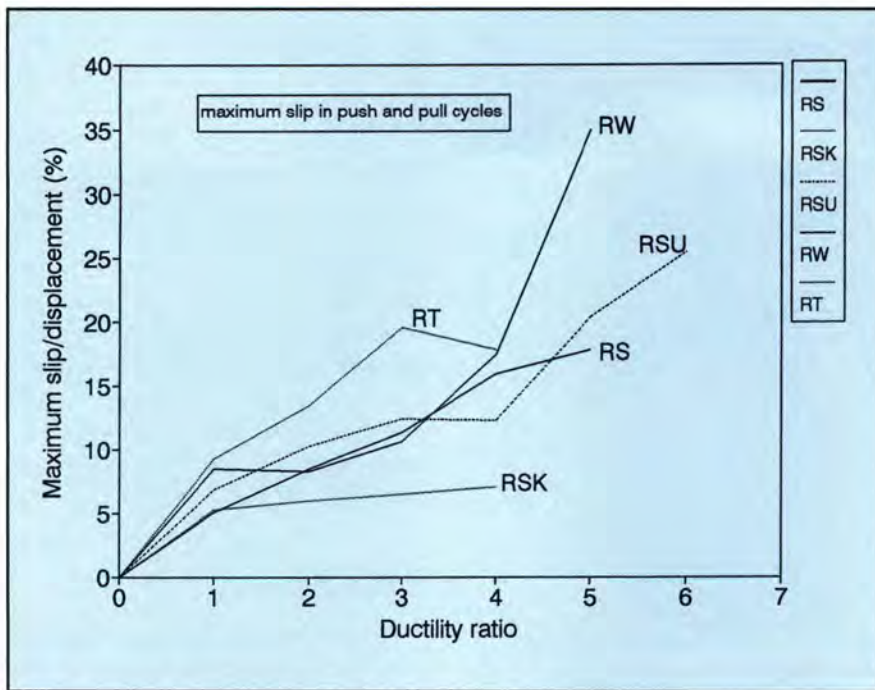


Fig. 6. Slip-to-displacement ratio at different ductility levels.



Fig. 7(a). Failure mode for Specimen RSU.

out of the bar from the sleeve at the first cycle of $7\Delta_y$. Cracking of the wall panels occurred at the end region of the connection.

Specimen RW failed at a drift of 1.39 percent and ductility ratio of 5. The extent of damage of Specimen RW at failure was similar to that of Specimen RSU with severe drypack crushing and spalling along the entire connection length. Cracking of the concrete wall panels at both connec-

tion ends was observed. Buckling of the compression reinforcement and rupture of tension reinforcement occurred at failure.

Specimen RSK had moderate damage and failed at a drift of 1 percent and ductility ratio of 5 by pull-out of the bar from the sleeve. The drypack crushing and spalling was moderate and was concentrated over one-sixth of the connection length from both ends of the connection. No damage or

only minor damage was observed in the shear keys, which remained intact, as shown in Fig. 7(b).

Specimen RT failed at a drift of 1 percent and at the first cycle of $5\Delta_y$. Severe crushing and spalling of the drypack at the connection extreme end and within the tube section was observed, as shown in Fig. 7(c). Local buckling of the tube section due to shear deformations also occurred. Vertical compression-type cracks were noted in the wall panels.

Connection Strength

The connection strength was determined based on the maximum load measured at the top of the upper panel and is given in Table 2 for all the connections. Variability of the strength among the different configurations, with the exception of Connection RT, was less than 14 percent.

The strength of Connection RT was 25 percent lower than Connection RS due to the flexibility and the low strength characteristics of the selected HSS steel tube vs. the sleeve or welded connector used for the other types of connections.

Connection Ductility

All mild steel specimens were capable of maintaining their maximum resistance under large cyclic displacement increments well beyond their first yield displacement. The deformability of the connection is expressed in terms of the ductility and the drift at failure.

Table 2 gives the ductility and drift percentage for all tested specimens. Connection RS-S, with sleeves, tested under monotonic loading had a ductility of 9 and a drift of 2 percent. The companion Connection RS tested under cyclic loading achieved a ductility of 5 and a drift of 1.18 percent. The welded Connection RW had a ductility of 5 and a drift of 1.39 percent. The lowest ductility of 4 and drift of 1 percent were measured for the shear key Connection RSK and the tube Connection RT. Specimen RSU, with unbonded reinforcement, had the highest ductility of 6 and a drift of 2.16 percent.



Fig. 7(b). Failure mode for Specimen RSK.



Fig. 7(c). Failure mode for Specimen RT.

Connection Stiffness

Stiffness degradation at service was monitored by means of the service load cycle, which was applied after each displacement increment. Stiffness of the connection was determined as the slope of peak-to-peak of the load-displacement hysteresis relationship following each displacement increment.

Fig. 8 compares stiffness degradation for the connections tested under cyclic loading in terms of the ratio of

measured stiffness, K , to the stiffness at yield, K_y , for different ductility levels. Fig. 8 shows that all connections had similar sharp stiffness degradation responses.

The initial stiffness at yield, K_y , is given in Table 2 and varies from 34 kN/m (2400 lbs per linear ft) for Connection RSU to 50 kN/m (3426 lbs per linear ft) for Connection RS.

The residual stiffness at failure, K_u , was approximately 25 percent of the stiffness at yield, K_y , as shown in Fig. 8 and given in Table 2. Such a de-

crease in stiffness seems to be a characteristic of degrading systems and has been observed by other researchers.¹ This loss of stiffness is due to progressive deterioration of drypack through crushing and spalling under the effect of cyclic loading conditions.

Energy Dissipation

Energy dissipation per cycle is calculated as the area enclosed by the load-displacement hysteresis loop. The cumulative energy dissipation is the summation of all the energy dissipation per cycle. Test results indicate that the cumulative energy dissipation is nonlinear for all the connections, as shown in Fig. 9. The results indicate that the cumulative energy dissipation for the plain connections was found to be higher than the shear key connection at failure due to their higher deformation capacity.

The welded connection had higher energy dissipation capacity than the mechanically spliced configuration. The steel tube coupler was found to have the lowest energy dissipation characteristic, which is due to premature failure of the tube. The unbonded connection had, by far, the best energy dissipation characteristics in comparison to all other configurations.

DISCUSSION OF TEST RESULTS

Effect of Reversed Cyclic Loading

Cyclic loading introduces a significant limit state due to the progressive deterioration of drypack, which is typically not observed in the behavior of the connection tested under monotonic loading conditions. The deterioration occurred initially as localized crushing in the compression zone, due to flexural compressive stresses, followed by an overall crushing along the entire length of the connection due to the grinding action.

The degree of deterioration varied depending on the connection configuration, as discussed earlier. The strength envelope of the hysteresis loops of Connection RS is compared to that of the companion Connection

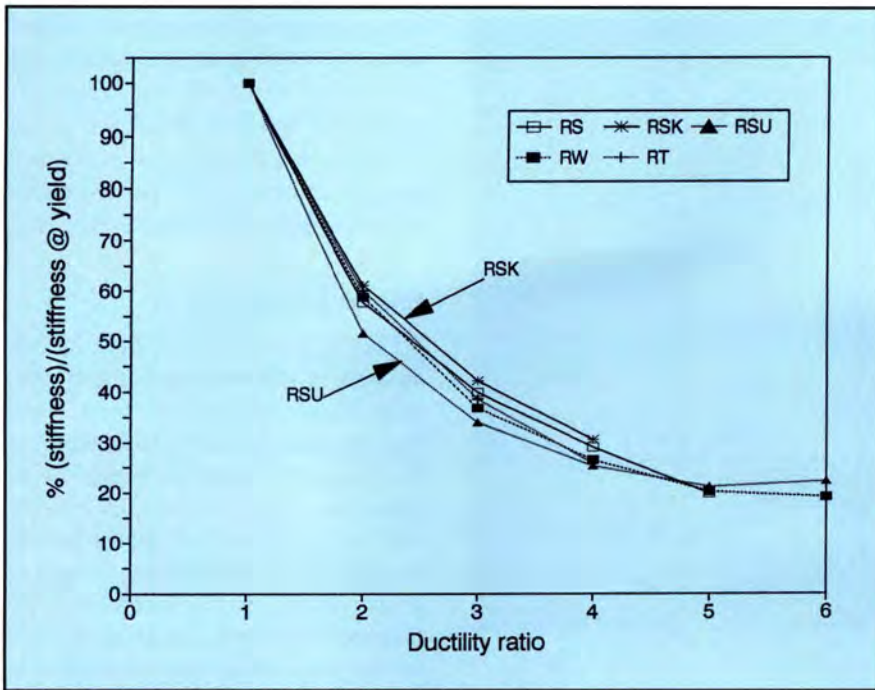


Fig. 8. Stiffness degradation for mild steel connections.

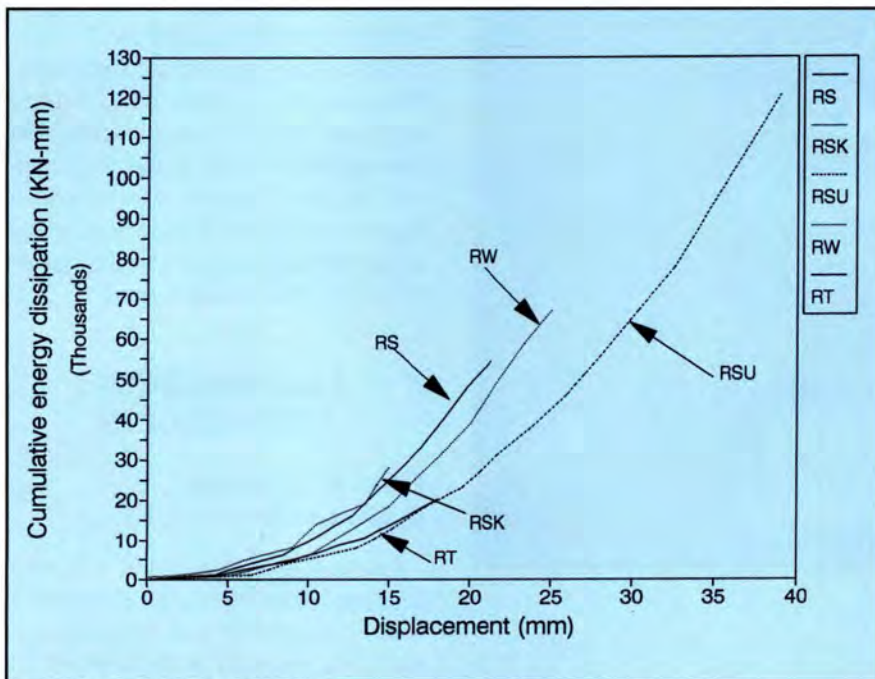


Fig. 9. Cumulative energy dissipation for mild steel connections.

RS-S tested under monotonic loading, as shown in Fig. 10.

As is evident from Fig. 10, cyclic loading did not affect the maximum measured strength. Cyclic loading, however, significantly reduced the ductility ratio from 9 for the connection tested under monotonic loading to a ductility ratio of 5. The cyclic loading also caused a sharp degradation in

the connection stiffness, as is evident by the significant reduction of the ratio of stiffness at ultimate to that at first yield (K_u/K_y) given in Table 2.

Effect of Shear Keys

The presence of shear keys prevented the extensive slip that occurred in the plain surface connections. The slip was

limited to 6 percent of the total deformation at all ductility levels. The shear resistance was provided by direct bearing of the strut formed within the keys to the concrete panels. This was evident in the initiation of hairline diagonal cracks within the keys.

The load-slip hysteresis loops were narrow and the slip was fully recoverable at zero displacement in contrast to "fat" and irrecoverable loops for the plain surface connection.

The overall response of the two connections is compared in Fig. 11. Both connections had similar strength and stiffness. However, the deformation capacity connection with shear keys was 20 percent lower than that of the plain surface connection, as is evident in Fig. 11.

Effect of Unbonding of Reinforcement

Unbonding of reinforcement is a new approach for shear wall connections to enhance the performance of the connection for seismic zones.

The most significant observed effect of unbonding of the reinforcement is the enhancement of deformation capacity without significant loss in strength, as shown in Fig. 11. The deformation capacity of the unbonded Connection RSU is almost doubled (1.8 times) in comparison to the bonded Connection RS. It should also be noted that the yield displacement of the unbonded specimen was 50 percent higher than the bonded specimen.

As a result of the higher deformation capacity, the degree of damage in the unbonded connection was more severe. The reduction in the thickness of the drypack was 5 percent, similar to the bonded specimen at the same deformation level. However, at failure, the thickness reduction was 35 percent for the unbonded specimen.

The hysteresis loops of the unbonded connection were slightly narrower and consequently less energy is dissipated per cycle for the unbonded vs. the bonded connection at any given displacement. The cumulative energy dissipation of the unbonded connection was significantly higher than the bonded connection due to its higher deformation capacity.

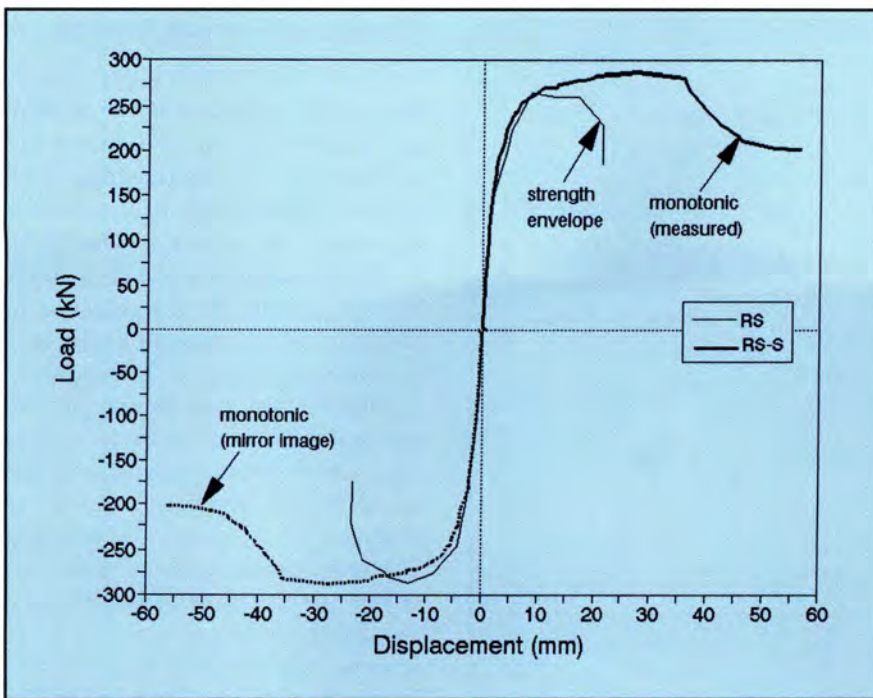


Fig. 10. Effect of cyclic loading.

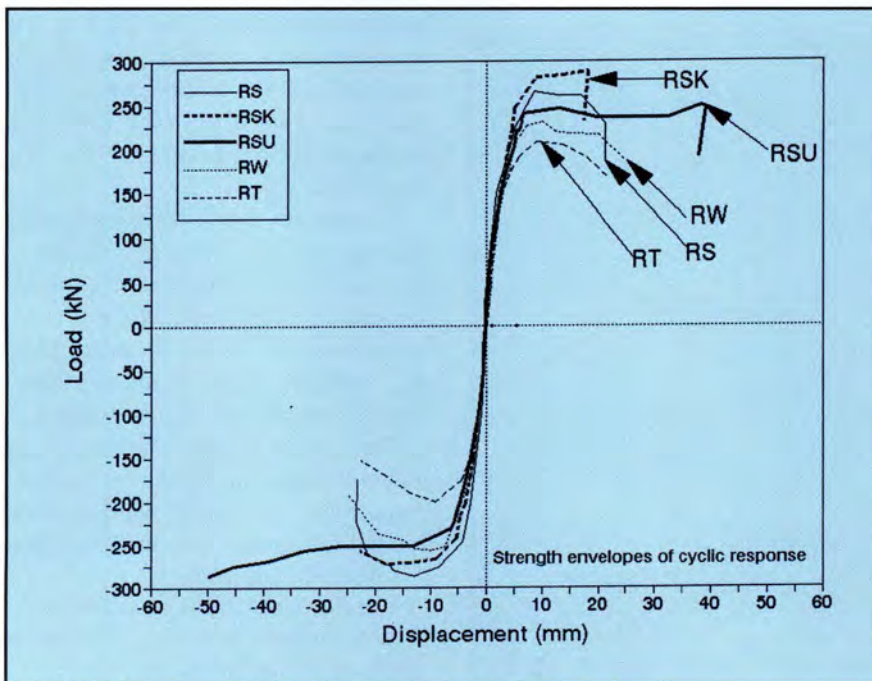


Fig. 11. Comparison of strength envelopes of cyclic response.

Welded vs. Splice Sleeve Connector

Both the welded and the sleeve connection showed similar response characteristics in terms of stable hysteretic behavior and ability to maintain their resistance at large deformations. The overall envelope of the response is compared in Fig. 11.

The absolute deformation capability of the welded Connection RW is about 20 percent higher than the sleeve Connection RS because the yield displacement was 20 percent higher than the sleeve connection. Therefore, the welded connection exhibited more severe deterioration before failure. However, both connections achieved a ductility ratio of 5. Reduction of the

thickness of the drypack was limited to 5 percent only for the splice sleeve connection and was up to 45 percent for the welded connection.

As a result of the severe deterioration and the flexibility of the welded steel angle vs. the splice sleeve detail, the slip-to-displacement ratio of the welded connection was about 35 percent in comparison to 20 percent for the sleeve connection. Energy dissipation for the welded connection was consistently 20 percent higher than for the splice sleeve connection.

Sleeve vs. Steel Tube Connector

The overall response of the steel tube Connection RT to the splice sleeve Connection RS is shown in Fig. 11. The strength of Connection RT was 25 percent lower than that of Connection RS. Also, the deformation capacity of the tube connection, was 20 percent lower than that of the sleeve connection. The lower strength and deformability were mainly due to the premature failure of the tube by local buckling and shear deformation of its vertical walls.

Severe drypack crushing concentrated at the ends of the connection for both types of connections. Reduction of the drypack thickness was limited to 5 percent for the sleeve connection and 3 percent for the tube connection. The energy dissipation for the tube connection was consistently 30 percent lower than for the sleeve connection, mainly due to flexibility of the tube. Therefore, it is important to design the tube to provide adequate strength, deformation, and energy dissipation needed for this type of connection. The design should prevent localized failure of the tube before failure of the continuity bars.

PROPOSED DESIGN PROCEDURE

A simplified design procedure was developed to predict strength and deformation for the described connections recommended for precast shear walls in seismic zones using the material characteristics used in the connection.

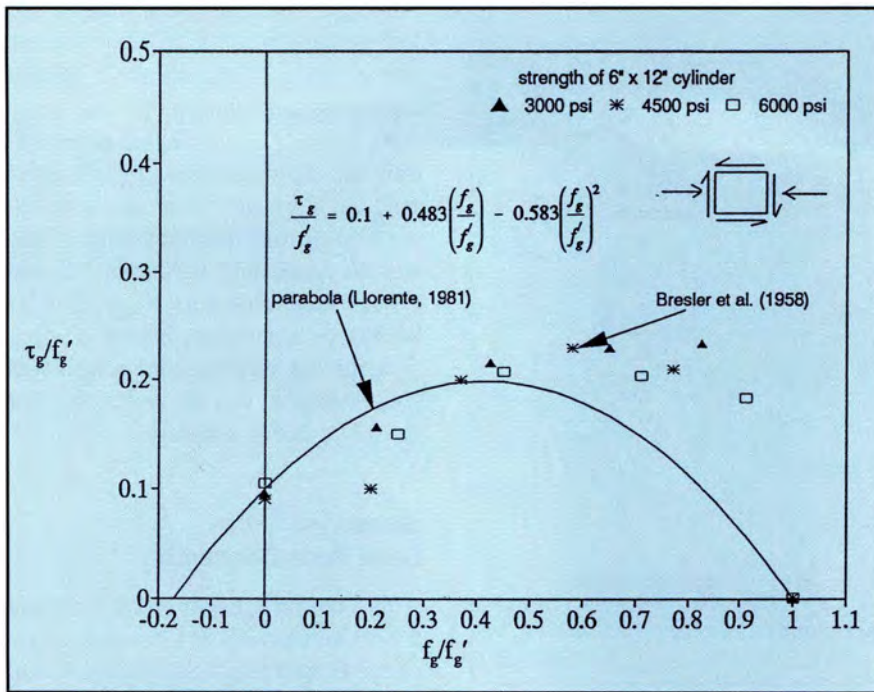


Fig. 12. Compression-shear interaction diagram.

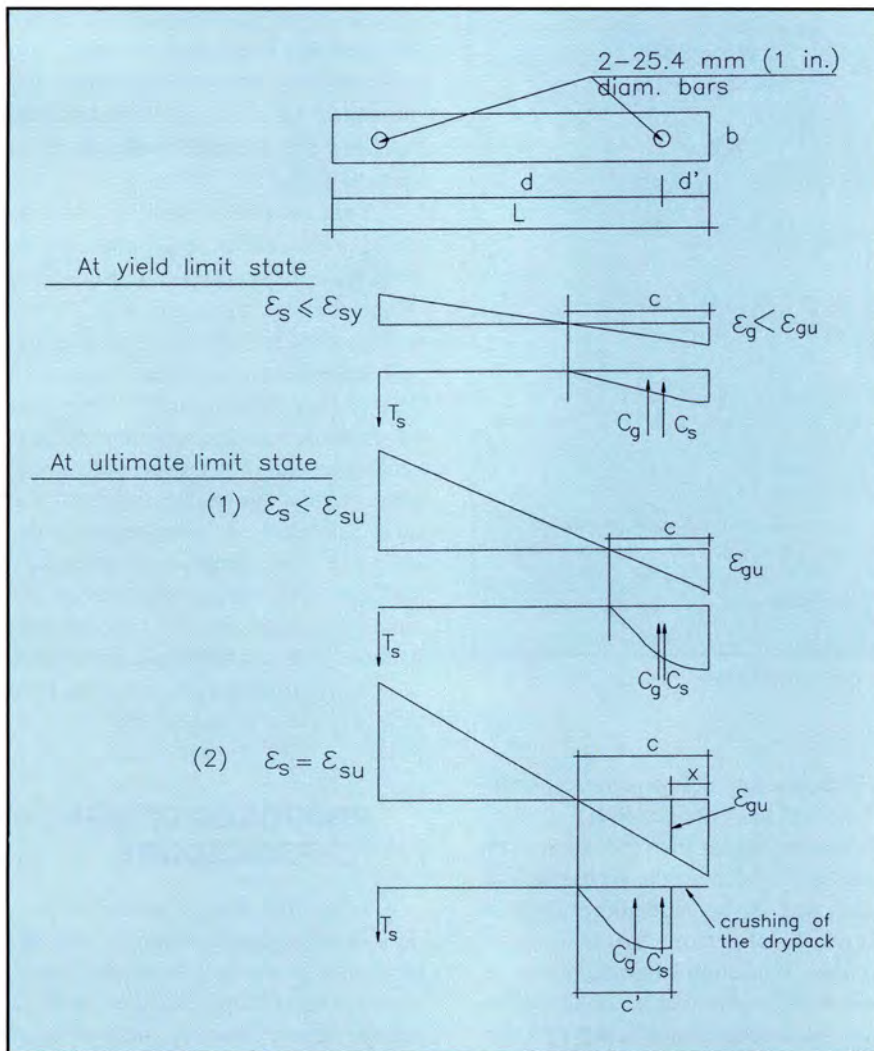


Fig. 13. Connection equilibrium and compatibility at various limit states.

Connection Flexural Strength

The flexural strength of the connection can be predicted using an iterative procedure based on equilibrium and compatibility. For a given strain in the tension reinforcement, ϵ_s , the analysis determines the neutral axis length, c , based on equilibrium and compatibility and accounts for the reduction in the compressive strength of the drypack due to presence of shear stresses.

The reduction, η , in the compressive strength of the grout can be determined from the interaction envelope of the compressive stresses f_g and shear stresses τ_g at the connection interface. The compression-shear interaction envelope used in this study is based on a parabolic envelope proposed by Llorente⁷ that provided a conservative fit for the measured data by Bresler and Pister,⁸ as shown in Fig. 12.

Three limit states of the connection response should be considered in the analysis, as shown in Fig. 13. The first state represents the elastic response up to yielding of the continuity bar in tension at a strain of ϵ_{sy} while the strain in the drypack is lower than the ultimate value, ϵ_{gu} .

At ultimate, two limit states should be considered. The first corresponds to the case when the extreme fiber of the connection reaches the ultimate compression strain of the drypack grout, ϵ_{gu} , while the strain in the reinforcement is less than the ultimate value, ϵ_{su} .

The second limit is when the strain in reinforcement reaches the maximum value, ϵ_{su} , causing shifting of the neutral axis away from the edges due to crushing of drypack.

The flowchart of the proposed iterative procedure, including the above limits, is shown in Fig. 14.

It should be mentioned that the ultimate strain of the drypack, ϵ_{gu} , was found to be in the range of 0.005 to 0.007 in this study. Therefore, an average value of 0.006 is recommended for design purposes.

Connection Deformation

Because of the inherently low stiffness of the drypack material in comparison to the concrete typically used for precast shear wall panels, it was observed that the top wall panel ro-

tates in rigid body motion with respect to the bottom panel. All the deformation was concentrated within the vicinity of the joint region and, therefore, flexural and shear deformations within the panels could be neglected. Total deformation of the top fiber of upper wall panel, Δ , could be expressed as a combination of slip deformation, Δ_s , and rocking deformation, Δ_r , as shown in Fig. 15:

$$\Delta = \Delta_s + \Delta_r \quad (1)$$

The magnitude of slip deformation is difficult to quantify even for the specimens tested in pure shear experiments.⁹ Past studies^{10,11,12} have reported that slip along horizontal connections is an unconfined mechanism with no restoring force and should be prevented.

The flexural deformation, Δ_r , is given in terms of the rotation, θ , and the height of the wall panel above the connection, H , as follows:

$$\theta = \frac{\Delta_r}{H} = \frac{\delta_s}{d - c} \quad (2)$$

where

d = distance from reinforcement in tension to extreme edge of connection in compression

c = compression zone depth from extreme edge of connection

δ_s = extension of reinforcement

In the vicinity of the connection, the continuity reinforcement develops elastic and plastic strain regions, as shown in Fig. 16.¹³ The strain distribution varies linearly from zero to the yield strain value within the elastic region, l_e . In the plastic region, l_p , the strain distribution is assumed to vary parabolically from the yield strain, ϵ_{sy} , to the maximum strain, ϵ_{sp} , value.

The extension of the reinforcement, δ_s , can be determined by integration of the strains along the bar in tension, as shown in Fig. 16, in the upper and lower panel on both sides of the connection region. Two cases should be identified depending whether the reinforcing bar is fully bonded or partially unbonded along a length l_u :

1. Bonded connection

At yield:

$$\delta_s = 2 \left(\frac{1}{2} \epsilon_{sy} l_e \right) \quad (3)$$

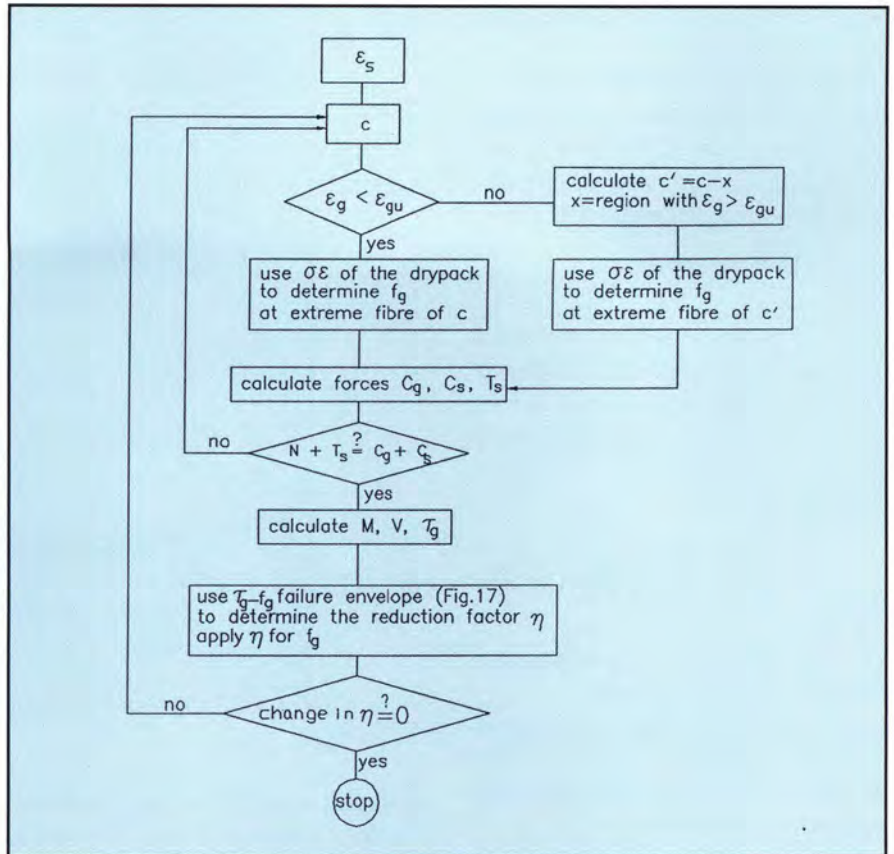


Fig. 14. Flowchart for flexural strength prediction.

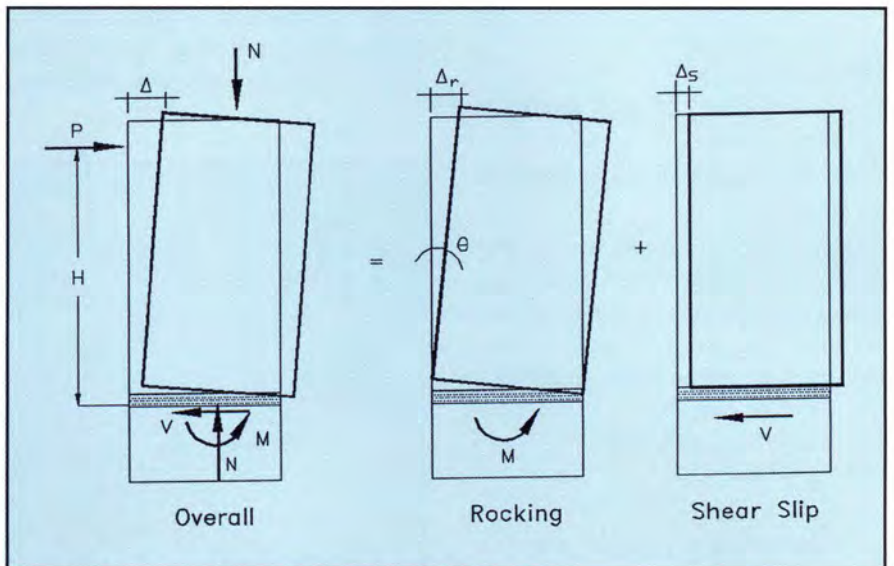


Fig. 15. Components of deformation: (a) rocking; (b) slip.

At ultimate:

$$\delta_s = 2 \left[\frac{1}{2} \epsilon_{sy} l_e + \epsilon_{sy} l_p + \frac{1}{3} (\epsilon_{sp} - \epsilon_{sy}) l_p \right] \quad (4)$$

2. Unbonded connection

At yield:

$$\delta_s = 2 \left(\frac{1}{2} \epsilon_{sy} l_e \right) + \epsilon_{sy} l_u \quad (5)$$

At ultimate:

$$\delta_s = 2 \left[\frac{1}{2} \epsilon_{sy} l_e + \epsilon_{sy} l_p + \frac{1}{3} (\epsilon_{sp} - \epsilon_{sy}) l_p \right] + \epsilon_{sp} l_u \quad (6)$$

where

ϵ_{sy} = yield strain of reinforcement

ϵ_{sp} = ultimate tensile strain of reinforcement

In general, the embedment length, l , at any stage depends on the bond stresses, u , of the reinforcement, bar diameter, d_b , and stress increment, Δf_s , in the reinforcement, as follows:

$$l = \frac{\Delta f_s d_b}{4u} \quad (7)$$

In the elastic region, the bond strength, u_e , is uniformly distributed along the length l_e , as shown in Fig. 16(b), and could be estimated using the ACI Code equation as given by French et al.¹⁴

$$u_e = 16 \frac{\sqrt{f'_c}}{d_b} \quad (\text{MPa}) \quad (8)$$

where f'_c is the uniaxial compressive strength of concrete in MPa.

In the plastic region, the bond strength, u_f , could be estimated using the expression proposed by Pochanart and Harmon¹⁵ as follows:

$$u_f = \left(5.5 - 0.07 \frac{S_b}{H_b} \right) \sqrt{\frac{f'_c}{28}} \quad (\text{MPa}) \quad (9)$$

where

S_b = clear spacing of lugs of reinforcement in mm

H_b = height of lugs of reinforcement in mm

In this program, the measured ultimate strain of the reinforcement, ϵ_{su} , under reversed cyclic loading was limited to 40 percent of the uniaxial tensile strain measured under monotonic loading. This conforms with the findings of Paulay and Priestley¹⁶ and Hawkins et al.¹⁷

DESIGN EXAMPLES

Two practical examples are given to illustrate how the proposed design procedure could be used to predict the response of various connections subjected to cyclic loading conditions. The first example predicts the response of a connection with bonded reinforcement and the second example gives the response of a partially unbonded reinforcement connection.

The connection selected has the same dimensions as the tested speci-

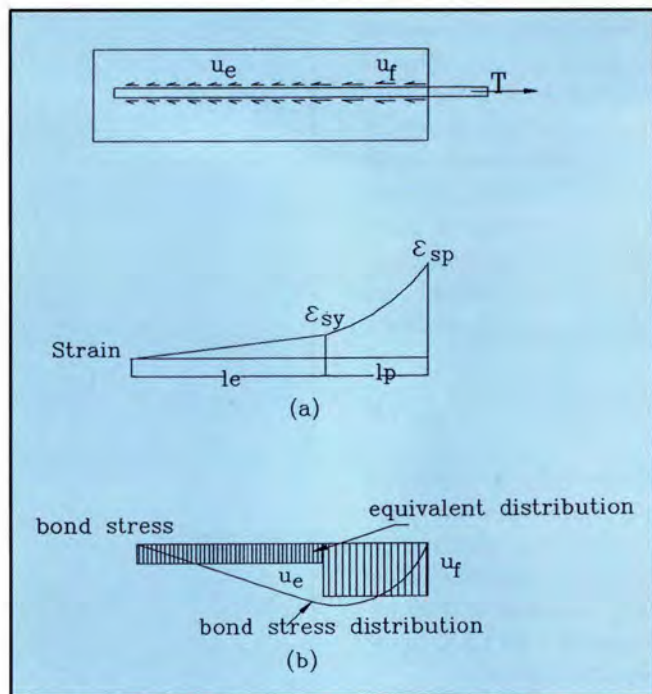


Fig. 16. Extension of continuity reinforcement.

mens and simulates a typical connection for a precast concrete loadbearing interior shear wall panel at the base of a 10-story building.

The connection geometry is shown in Fig. 17 and is 1200 mm (47.25 in.) long and 152 mm (6 in.) wide with a 20 mm (0.78 in.) drypack thickness.

The continuity between the two panels is provided by two 25.4 mm (1 in.) diameter Grade 400 MPa (60 ksi) mild steel reinforcing bars spaced at 900 mm (35.4 in.) on center. The distance from the tension steel to the extreme compression fiber, d , is 1050 mm (41.3 in.) and the distance from the compres-

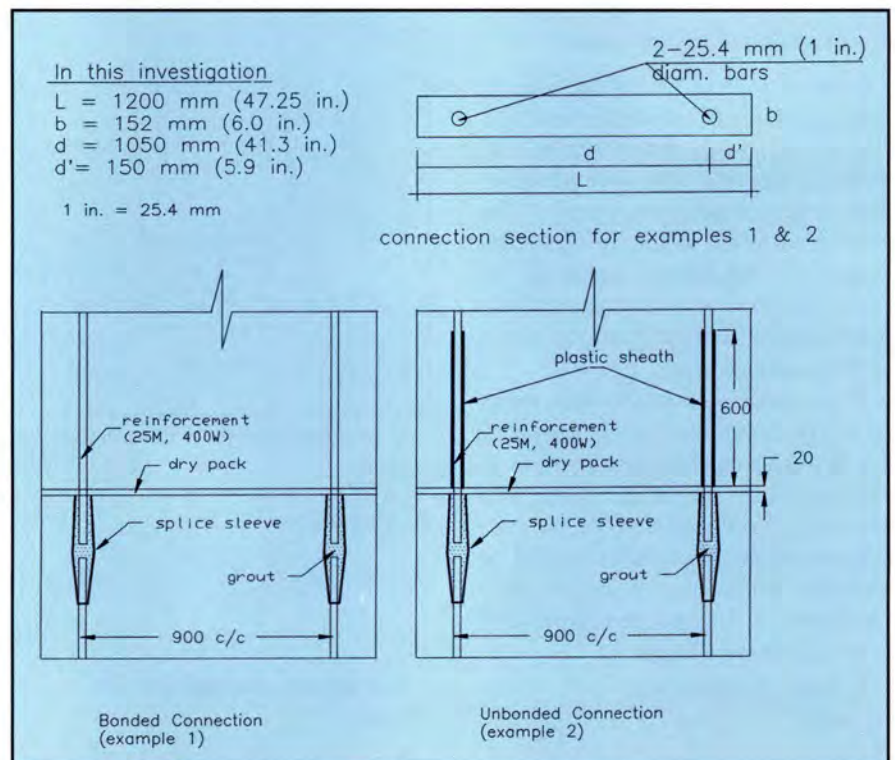


Fig. 17. Connection dimensions used in design examples.

sion steel to the extreme compression fiber, d' , is 150 mm (5.9 in.). The pressure of the weight of nine stories above the connection is 2 MPa (0.29 ksi).

The characteristic properties of the different materials used in the connection are:

Concrete:

Cylinder compressive strength,
 $f'_c = 45$ MPa (6.52 ksi)

Drypack:

Cube compressive strength,
 $f'_g = 57$ MPa (8.26 ksi)

Cylinder compressive strength,
 $f'_g = 0.85f'_g = 48$ MPa (6.96 ksi)

Ultimate compressive strain,
 $\epsilon_0 = 0.006$

Mild reinforcing steel:

Area of one bar,
 $A_s = 500$ mm² (0.77 sq in.)

Yield strength,
 $f_{sy} = 400$ MPa (58 ksi)

Yield strain, $\epsilon_{sy} = 0.0023$

Young's modulus of elasticity,
 $E_s = 200000$ MPa (29,000 ksi)

Ultimate tensile strength,
 $f_{su} = 650$ MPa (94.27 ksi)

Ultimate strain under static load,
 $\epsilon_{su} = 0.090$

Ultimate strain under cyclic load
($0.40\epsilon_{su}$ static), $\epsilon_{su} = 0.036$

Example 1: Bonded Connection

This example predicts the envelope of response of bonded mild steel reinforcement connection subjected to cyclic loading condition.

Response at yield — The flexural strength at yield can be determined using the flowchart shown in Fig. 14. The analysis converges to a compression zone length of 380 mm (14.9 in.) and a compressive strain in the drypack at the extreme compression fiber of the connection of 0.0013, which is less than the ultimate.

The corresponding flexural resistance at yield is 352 kN-m (260 kip-ft). The equilibrium and compatibility are satisfied with a reduction factor, η , for the drypack compressive strength of 0.88, which corresponds to a shear stress of 3.45 MPa (0.5 ksi).

The rotation of the connection can

be determined based on the extension of the continuity reinforcement.

The bond strength, u_e can be determined using Eq. (8):

$$u_e = 16 \frac{\sqrt{45}}{25.4} \\ = 4.23 \text{ MPa (0.62 ksi)}$$

The elastic length l_e on either side of the connection can be determined using Eq. (7):

$$l_e = \frac{400 \times 25.4}{4 \times 4.23} \\ = 601 \text{ mm (23.6 in.)}$$

Therefore, the bar extension, δ_s , can be determined using Eq. (3):

$$\delta_s = 2 \times \frac{1}{2} \times 0.0023 \times 601 \\ = 1.38 \text{ mm (0.0543 in.)}$$

The rotation, θ , can be evaluated using Eq. (2):

$$\theta_y = \frac{1.38}{1050 - 380} = 0.0020$$

Response at ultimate — Two limit states are considered at ultimate, as shown in Fig. 13.

1. Limit State 1 — This limit state corresponds to the case when the strain in the extreme fiber of the connection reaches the ultimate compression strain of the drypack grout, ϵ_{gu} , while the strain in the tension reinforcement is less than ϵ_{su} .

For a strain of 0.006 at the extreme fiber of the connection, the analysis converges to a compression zone length of 190 mm (7.48 in.) and a strain, ϵ_{sp} , of 0.027 in the tension reinforcement. This strain is less than the ultimate value of 0.036 under reversed cyclic loading. The strength of the connection at this stage is determined from equilibrium conditions and is equal to 458 kN-m (337.8 kip-ft). The compression strength reduction factor, η , is 0.57, determined from the failure envelope for shear stress of 8.7 MPa (1.26 ksi).

To determine the rotation at the connection using extension of reinforcement, the frictional bond strength in the plastic region can be determined from Eq. (9):

$$u_f = (5.5 - 0.07) \frac{8}{2} \sqrt{\frac{45}{28}} \\ = 6.6 \text{ MPa (0.96 ksi)}$$

The plastic zone l_p can be determined using Eq. (7):

$$l_p = \frac{(560 - 400)(25.4)}{(4)(6.6)} \\ = 154 \text{ mm (6.07 in.)}$$

Extension of the bar, δ_s , can be determined from Eq. (4):

$$\delta_s = 2 \left[\frac{1}{2} (0.0023)(600) + (0.0023)(154) + \frac{1}{3} (0.027 - 0.0023)(154) \right] \\ = 4.63 \text{ mm (0.183 in.)}$$

The rotation at ultimate limit state 1, θ_u , can be evaluated using Eq. (2):

$$\theta_{u1} = \frac{4.63}{1050 - 190} = 0.0054$$

2. Limit State 2 — This state considers the case when the strain in the reinforcement reaches the ultimate value, ϵ_{su} , and the strain of the extreme fiber is greater than the ultimate compression strain of the grout, ϵ_{gu} . This case will cause a shifting of the neutral axis away from the edge of the connection due to crushing of the drypack.

Based on an ultimate strain, ϵ_{su} , of 0.0036, the analysis converges to a compression zone depth, c , of 220 mm (8.67 in.) within which the drypack strain exceeds the ultimate along a length of 73 mm (2.874 in.) and the compression stresses are distributed along a length, c' , of 147 mm (5.78 in.) from the neutral axis.

The analysis indicates that the drypack strain at the extreme fiber is 0.09, which is greater than the ultimate value of 0.006. The reduction of the grout compressive strength is 0.55 and the flexural strength of the connection is 415 kN-m (306 kip-ft).

The plastic zone depth l_p can be determined using Eq. (7):

$$l_p = \frac{(600 - 400)(25.4)}{(4)(6.6)} \\ = 193 \text{ mm (7.6 in.)}$$

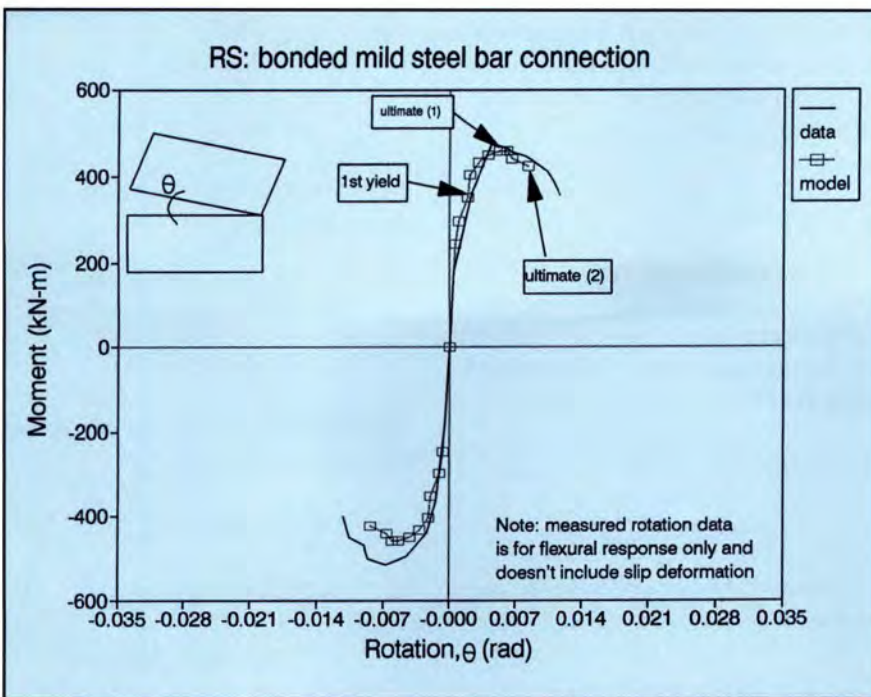


Fig. 18. Comparison of predicted vs. measured response for bonded connection.

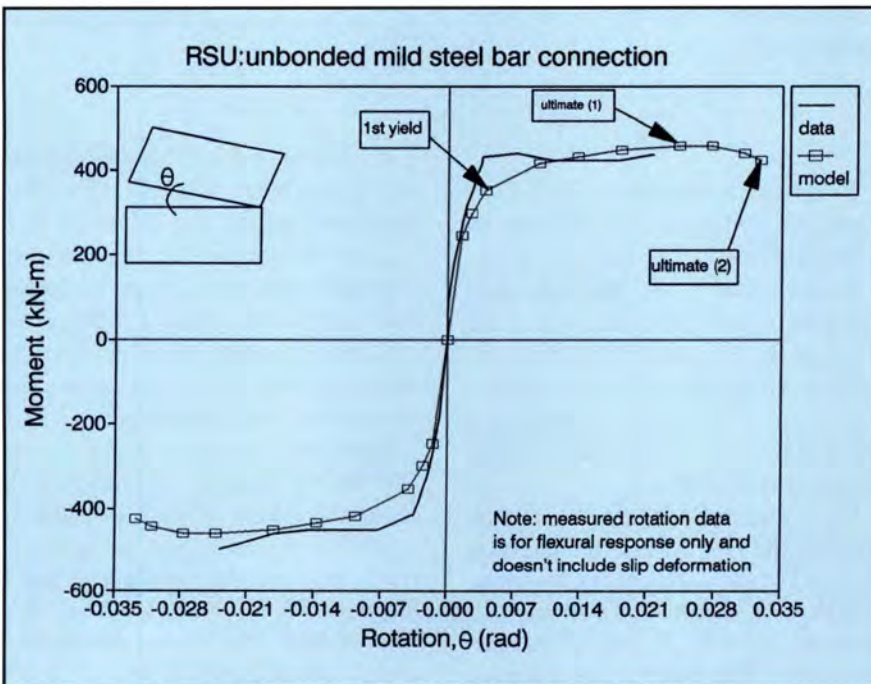


Fig. 19. Comparison of predicted vs. measured response for unbonded connection.

Extension of the bar, δ_s , can be determined from Eq. (4):

$$\begin{aligned} \delta_s &= 2 \left[\frac{1}{2}(0.0023)(601) + \right. \\ &\quad (0.0023)(193) + \\ &\quad \left. \frac{1}{3}(0.036 - 0.0023)(193) \right] \\ &= 6.60 \text{ mm (0.26 in.)} \end{aligned}$$

The rotation at ultimate state 2, θ_u , can be evaluated using Eq. (2):

$$\theta_{u2} = \frac{6.6}{1050 - 220} = 0.008$$

Other points of the moment-rotation response are determined using a computer spreadsheet following the same procedure described in Fig. 14. The complete predicted response is in ex-

cellent agreement with the measured flexural response, as shown in Fig. 18, excluding the slip deformation for Connection RS.

Example 2: Unbonded Connection

This example predicts the envelope of response of a partially unbonded mild steel reinforcement connection subjected to cyclic loading. In this example, the unbonded length of the bar, l_u , is selected to be 600 mm (23.6 in.) above the joint region in the upper panel.

Response at yield — At yield, the entire unbonded length, l_u , of the reinforcing bar will yield. For the given yield strain of 0.0023, the analysis gives a compression zone length of 380 mm (14.96 in.) and a resultant moment of 352 kN-m (260 kip-ft), as presented earlier in Example 1.

Calculation of the rotation at yield is based on extension of the reinforcement, δ_s , which is determined for the unbonded connection using Eq. (5):

$$\begin{aligned} \delta_s &= 2 \left[\frac{1}{2}(0.023)(601) \right] + (0.023)(600) \\ &= 2.76 \text{ mm (0.10 in.)} \end{aligned}$$

The rotation of the joint, θ , can be determined using Eq. (2):

$$\theta_y = \frac{2.76}{1050 - 380} = 0.004$$

Response at Ultimate

1. Limit State 1 — For a strain of 0.006 at the extreme fiber, the analysis converges to a compression zone length of 190 mm (7.48 in.) and a flexural resistance of 458 kN-m (337.8 kip-ft).

The extension of the reinforcement, δ_s , can be determined from Eq. (6):

$$\begin{aligned} \delta_s &= 2 \left[\frac{1}{2}(0.0023)(600) + \right. \\ &\quad (0.0023)(154) + \\ &\quad \left. \frac{1}{3}(0.027 - 0.0023)(154) \right] + \\ &\quad (0.027)(600) \\ &= 20.83 \text{ mm (0.82 in.)} \end{aligned}$$

The rotation at ultimate limit state 1, θ_{u1} , can be evaluated using Eq. (2):

$$\theta_{u1} = \frac{20.83}{1050 - 190} = 0.024$$

2. Limit state 2 — Based on an ultimate strain, ϵ_{su} , of 0.0036, the analysis converges to a compression zone depth, c , of 220 mm (8.67 in.) and a flexural strength of 415 kN-m (306 kip-ft).

The extension of the bar, δ_s , can be determined from Eq. (6):

$$\begin{aligned} \delta_s &= 2 \left[\frac{1}{2}(0.0023)(601) + \right. \\ &\quad (0.0023)(193) + \\ &\quad \left. \frac{1}{3}(0.036 - 0.0023)(193) \right] + \\ &\quad (600)(0.036) \\ &= 28 \text{ mm (1.10 in.)} \end{aligned}$$

The rotation at ultimate state 2, θ_{u2} , can be evaluated by use of Eq. (2):

$$\theta_{u2} = \frac{28}{1050 - 220} = 0.033$$

The complete predicted response is in excellent agreement with the measured flexural response, excluding slip deformation for Connection RSU, with identical configuration to the example, as shown in Fig. 19.

It should be mentioned that in both examples no attempt was made to quantify the slip because slip represents an unconfined mechanism and should be avoided.

CONCLUSIONS

All five mild steel connections for the precast concrete panel wall system investigated behaved satisfactorily under reversed cyclic loading with

ductility and energy dissipation levels comparable to monolithic connections. Based on the results of this study, the following conclusions can be drawn:

1. The cyclic behavior of the connection can be identified by three limit states:

- Linear elastic stage before yielding
- Nonlinear ductile stage without significant deterioration with stable hysteresis
- Failure with significant deterioration of the drypack

2. A ductility of 4 could be achieved by all tested connections without any apparent damage to the connection. This level represents typical seismic demand for low to moderate seismicity.

3. All connections tested were capable of withstanding large nonlinear deformations well beyond first yield with very good energy absorption. The ductility ranged from 4 to 6.

4. The mode of failure for all connection configurations tested under cyclic loading was due to significant crushing and spalling of drypack. Crushing was accompanied by rupture or pull-out of the continuity reinforcement from the sleeve at the connection level.

5. Partial debonding of continuity reinforcement across the connection almost doubled the deformability capacity in comparison to the bonded connection without influencing the strength.

6. The presence of shear keys across the joint interface limited the slip mechanism, which is desirable in the overall response of precast shear wall connections.

7. The stiffness degradation was characterized by a sharp decrease of stiffness vs. ductility. The residual stiffness at onset of failure was about 25 percent of that at yield.

8. The proposed design models for

the strength and rotation capacity of typical and new connection configurations are in excellent agreement with the measured values.

RECOMMENDATIONS

1. Properly designed mild steel connections for precast wall panels exhibit sufficient ductility and energy dissipation capacity for use in seismic zones.

2. Debonding of the continuity reinforcement is recommended because it significantly enhances the connection response in terms of deformability and energy dissipation. The increase in connection deformability depends on the degree of debonding provided in the connection region. Also, at a given deformation, the unbonded connection has a lower energy dissipation per cycle and a higher cumulative energy dissipation in comparison to the bonded connection.

3. The use of shear keys across the interface of the connection significantly limits the slip mechanism and enhances the shear resistance. This behavior is desirable in seismic zones because shear slip is an unconfined mechanism with no restoring force and should be prevented. Therefore, shear keys are recommended at the interface of precast connections.

ACKNOWLEDGMENT

This experimental program was conducted at the University of Manitoba, Canada, with financial assistance from the Natural Sciences and Engineering Research Council of Canada (NSERC), Con-Force Structures Ltd., and Supercrete Ltd., Winnipeg, Manitoba. The help of graduate student Jeff West and laboratory technicians E. Lemke and M. McVey is greatly appreciated.

REFERENCES

1. Applied Technology Council, *Design of Prefabricated Concrete Buildings for Earthquake Loads*, ATC-8, Berkeley, California, 1981.
2. Stanton, J. F., and Nakaki, S. D., "PRESSS Industry Seismic Workshops," *PRESSS Research Reports 91/01, 91/02 and 92/06*, edited by M. J. N. Priestley, University of California at San Diego, San Diego, CA.
3. Soudki, K. A., "Behavior of Horizontal Connections for Precast Concrete Loadbearing Shear Wall Panels Subjected to Large Reversed Cyclic Deformations," Ph.D. Thesis, University of Manitoba, Winnipeg, Manitoba, Canada, May 1994, 670 pp.
4. Foerster, H. R., Rizkalla, S. H., and Huevel, J. S., "Behavior and Design of Shear Connections for Loadbearing Wall Panels," *PCI JOURNAL*, V. 34, No. 1, January-February 1989, pp. 102-119.
5. Serrette, R. L., Rizkalla, S. H., Attiogbe, E. K., and Huevel, J. S., "Multiple Shear Key Connections for Precast Shear Wall Panels," *PCI JOURNAL*, V. 34, No. 2, March-April 1989, pp. 104-120.
6. Hutchinson, R. L., Rizkalla, S. H., Lau, M., and Huevel, J. S., "Horizontal Post-Tensioned Connections for Precast Concrete Loadbearing Shear Wall Panels," *PCI JOURNAL*, V. 36, No. 6, November-December 1991, pp. 64-76.
7. Llorente, C. A., "Inelastic Behavior of Precast Shear Walls," Massachusetts Institute of Technology Department of Civil Engineering, Research Report No. R81-25, Order No. 710, August 1981.
8. Bresler, B., and Pister, K. S., "Strength of Concrete Under Combined Stresses," *ACI Journal*, V. 55, No. 3, September 1958, pp. 321-345.
9. West, J. S., "Behaviour of Horizontal Connections for Precast Concrete Load-Bearing Shear Wall Panels Subjected to Large Reversed Cyclic Shear Loading," MS Thesis, University of Manitoba, Winnipeg, Manitoba, Canada, August 1993, 319 pp.
10. Becker, J. M., Llorente, C., and Mueller, P., "Seismic Response of Precast Concrete Walls," *Earthquake Engineering and Structural Dynamics*, V. 8, No. 6, November-December 1980, pp. 545-564.
11. Mueller P., "Behavioral Characteristics of Precast Walls," Proceedings of a Workshop on Design of Prefabricated Concrete Buildings for Earthquake Loading, Applied Technology Council, April 1981, pp. 277-308.
12. Oliva, M. G., Clough, R. W., and Malhas, F., "Seismic Behavior of Large Panel Precast Walls: Analysis and Experiment," *PCI JOURNAL*, V. 34, No. 5, September-October 1989, pp. 42-67.
13. Park, R., and Paulay, T., *Reinforced Concrete Structures*, John Wiley & Sons, New York, NY, 1975.
14. French, C., Leon, R., and Grundhoffer, T., "Bond Behavior of Uncoated and Epoxy Coated Reinforcement in Concrete," Structural Engineering Report No. 92-04, University of Minnesota, Center of Transportation Studies, May 1992, 208 pp.
15. Pochanart, S., and Harmon, T., "Bond-Slip Model for Generalized Excitation Including Fatigue," *ACI Materials Journal*, V. 86, No. 5, September-October 1989, pp. 465-474.
16. Paulay T., and Priestley, M. J. N., *Seismic Design of Reinforced Concrete and Masonry Buildings*, John Wiley & Sons, New York, NY, 1991.
17. Hawkins, N. M., Lin, I., and Ueda, T., "Anchorage of Reinforcing Bars for Seismic Forces," *ACI Structural Journal*, V. 84, No. 5, September-October 1987, pp. 407-418.

APPENDIX — NOTATION

- | | | |
|--|--|---|
| A_s = area of reinforcement in tension
b = width of connection
c = compression zone depth from extreme edge of connection subjected to compression
c' = length within compression zone length, c , with ϵ_g less than ϵ_{gu}
d = distance from tension reinforcement to extreme edge of connection under compression
d' = distance from compression reinforcement to extreme edge of connection under compression
d_b = diameter of reinforcing bar
Δ = total displacement of top panel at location of applied load and relative to bottom panel
Δ_r = flexural (rocking) deformation measured at top panel at location of applied load
Δ_s = slip deformation at connection region
Δ_y = total displacement at first yield of continuity reinforcement
Δ_u = total displacement at ultimate | strain of continuity reinforcement
Δf_s = stress increment in bar due to applied load
δ_s = extension of continuity reinforcement
e = energy dissipation per cycle
E = cumulative energy dissipation
E_{ps} = Young's modulus of elasticity of continuity reinforcement
ϵ_{gu} = ultimate compressive strain of drypack
ϵ_{sy} = yield strain of continuity reinforcement
ϵ_{sp} = strain in reinforcement
ϵ_{su} = ultimate tensile strain of continuity reinforcement
f'_c = cylinder compressive strength of concrete at 28 days
f'_g = equivalent cylinder compressive strength of drypack at 28 days
f''_g = cube compressive strength of drypack grout
f_{sp} = stress in continuity reinforcement at strain ϵ_{sp} | f_{sy} = yield stress in reinforcement at yield strain, ϵ_{sy}
f_{su} = ultimate stress in reinforcement at ultimate strain, ϵ_{su}
H = height of upper panel above connection region
H_b = height of lugs of bar
K_y = stiffness at first yield
K_u = stiffness at ultimate
l_e = elastic embedment length of tension reinforcement
l_p = plastic embedment length of tension reinforcement
S_b = clear space of lugs of bar
S_u = slip at ultimate level
μ_Δ = ductility ratio of Δ_u to Δ_y
θ = rotation of connection
τ_g = shear stress within compression zone
u_e = elastic bond strength of bar within elastic zone
u_f = frictional bond strength of bar within plastic zone
x = length within compression zone length, c , with ϵ_g greater than ϵ_{gu} |
|--|--|---|